

Biodegradable and temperature-responsive thermoset polyesters with renewable monomers

XiauYeen Lee,¹ Mat Uzir Wahit,² Nadia Adrus¹

¹Department of Polymer Engineering, Faculty of Chemical and Energy Engineering, Universiti Teknologi Malaysia 81310, Skudai Johor, Malaysia

²Centre for Composite, Faculty of Mechanical Engineering, Universiti Teknologi Malaysia 81310, Skudai, Johor, Malaysia

Correspondence to: M. U. Wahit (E-mail: mat.uzir@cheme.utm.my)

ABSTRACT: A series of biodegradable thermoset polyesters, poly(1,8-octanediol–glycerol–dodecanedioate)s (POGDAs), were synthesized with the polycondensation polymerization method without a catalyst and with different monomer molar ratios. Synthesis was confirmed with structural analysis via Fourier transform infrared spectroscopy. The effect of varying the monomer molar ratio on the material properties was illustrated in the gel content and swelling analysis, ultraviolet–visible spectroscopy, differential scanning calorimetry, X-ray diffraction, and degradation tests. Degradation tests were performed in phosphate-buffered solution at 37 °C for 60 days. Temperature-responsive behavior was revealed with POGDA (0.5 glycerol), and bending tests were performed to study the shape-memory effect. *In vitro* cytotoxicity tests and cell proliferation tests suggested that these POGDAs have potential applications in biomedical fields such as tissue engineering. © 2016 Wiley Periodicals, Inc. *J. Appl. Polym. Sci.* **2016**, *133*, 44007.

KEYWORDS: biodegradable; biomaterials; polyesters; stimuli-sensitive polymers; thermosets

Received 17 February 2016; accepted 7 June 2016

DOI: 10.1002/app.44007

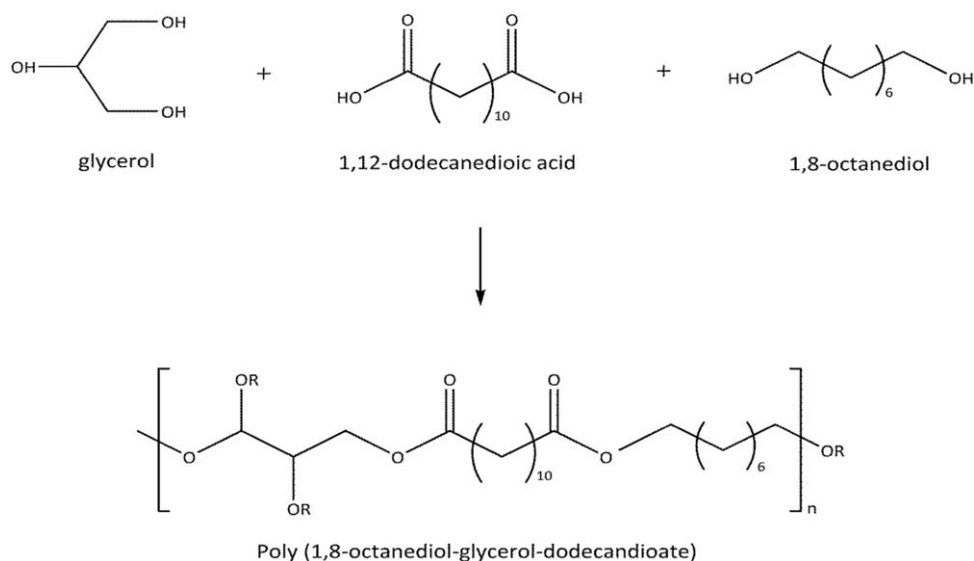
INTRODUCTION

Polymer-based biomaterials have been developed since the 1920s.¹ Market research reports by MarketsAndMarkets has indicated that the biomaterials market will be worth US\$130.57 billion by 2020. Polymeric biomaterials are the fastest growing field in biomaterials. The main reasons for the popularity of polymeric biomaterials are their low cost, ease of production, light weight, great mechanical strength, and biocompatibility. Biodegradable and biocompatible polymers have been considered as replacements for permanent prosthetic devices used for temporary treatments.^{2,3} The development of a new generation of synthetic biodegradable polymers is underway and is being driven by the latest biomedical technologies, such as tissue engineering and controlled drug delivery.^{4–6}

The consumption of polymeric biomaterials is more than 8000 kt annually, yet the market contains only a small fraction of degradable polymers.^{7,8} Public concerns about the environment have created an interest in biodegradable polymeric biomaterials synthesized from renewable resources. Attention has been paid to biodegradable polyesters that are easily produced from renewable resources such as poly(lactic acid), a thermoplastic polyester.^{9,10} Biodegradable thermoplastic polyesters degrade through bulk erosion, and this results in mechanical instability.^{11,12} Thermoset polyesters that degrade via surface

erosion were developed to improve mechanical stability.¹³ Thermoset polyesters are hydrolytically degradable, retain their mechanical integrity during degradation, and offer a wide range of properties that can be achieved through the manipulation of monomers and synthesis conditions.^{14,15} Different degrees of crosslinking densities in thermoset polyesters create different material properties for the same type of material.

Biodegradable polymers with smart functions, such as thermoresponsivity, have been reported in the area of petroleum-based polymers and include poly(ϵ -caprolactone), polyurethanes, and their copolymers.^{16–18} Few studies have been conducted on bio-based polymers.^{19–21} For thermally responsive or shape-memory polymers, there are two shapes in the shape-memory process, one permanent shape and another temporary shape. Hard segments determine the permanent shape of a polymer, whereas soft segments determine the temporary shape. Shapes can be switched at the transition temperature (T_{trans}). Deformation occurs above T_{trans} , and cooling below T_{trans} allows a shape-memory polymer to obtain a temporary shape. The permanent shape of a shape-memory polymer can be recovered through heating to above T_{trans} . The glass-transition temperature T_g or melting temperature (T_m) can be a T_{trans} ; this depends on the type of polymer.



Scheme 1. Reaction scheme between Oct, Gly, and DA to produce POGDA.

1,8-Octanediol (Oct) and glycerol (Gly) were used in this study to react with 1,12-dodecanedioic acid (DA) to form a thermoset polyester, poly(1,8-octanediol-glycerol-dodecanedioate) (POGDA). Oct is the longest water-soluble aliphatic diol, with no reported toxicity in research conducted by Yang *et al.*²² to produce poly(1,8-octanediol-co-citrate). Their research showed the potential of Oct as a monomer for the synthesis of polyesters for biomedical applications. A precursor to lipids, Gly is mainly produced from renewable resources as a byproduct during the transesterification of vegetable oils and animal fat in the production of biodiesel.^{23,24} It can also be produced by microbial fermentation.²⁵ DA has 12 carbon atoms²⁶ and a longer chain of dicarboxylic acid compared to adipic acid and glutaric acid. DA was chosen for this study because short-chain aliphatic dicarboxylic acids tend to stimulate intramolecular condensation.²⁷ DA can be produced from renewable resources, such as *vernonia galamensis* oil.²⁸

Monomers derived from renewable resources are potential raw materials for thermoset polyesters. With three monomers to create a long backbone chain for this study, the degree of crosslinking and crystallinity was manipulated through the variation of the monomer molar ratios. Only POGDA (0.5 Gly) exhibited excellent shape-memory behavior; this confirmed the role of crystallinity for the soft segments. All of the synthesized POGDAs were biodegradable and showed different material properties with different molar ratios. POGDA polymers showed comparable biocompatibilities with poly(lactic acid) (PLA), the commonly used material for biomedical application suggesting the potential application of POGDA in this field.

EXPERIMENTAL

Synthesis and Preparation of POGDA

High-purity Oct (molecular weight = 146.23 g/mol, $T_m = 57-61^\circ\text{C}$), Gly (molecular weight = 92.09 g/mol, $T_m = 20^\circ\text{C}$), and 1,12-dodecanedioic acid (molecular weight = 230.3 g/mol, $T_m = 127-129^\circ\text{C}$) were purchased from Sigma-Aldrich and were used as received.

POGDA was synthesized with the polycondensation polymerization method, which is also a solvent-free and catalyst-free method (Scheme 1). The synthesis of the prepolymer was carried out in a 500-mL, round-bottomed reaction flask with a reactant stoichiometry of 0.1:0.9:1 of Oct to Gly to DA under a dry nitrogen atmosphere. Amounts of 3.217 g of Oct and 50.666 g of DA powder were placed into the reaction flask, which was equipped with a mechanical stirrer, in a 140°C oil bath. After the solid Oct and DA melted completely, the reaction temperature was decreased to 120°C while 18.236 g of Gly was added to the flask. The solution was stirred continuously for 24 h to produce the prepolymer of POGDA. The synthesized prepolymer was cast into a preheated polytetrafluoroethylene mold ($16 \times 18 \times 1 \text{ mm}^3$) and cured for 7 days at 120°C in a universal oven. This was repeated with different molar ratios for Oct and Gly with DA. The synthesized POGDAs were washed with acetone to remove any unreacted monomers and kept in a desiccator after drying.

Formulation Development

Five samples were synthesized with different molar ratios of Oct and Gly to react with DA. The formulations and designations of POGDA are listed in Table I.

Structural Analysis

Fourier transform infrared (FTIR) spectra were obtained at ambient temperatures with a Spectrum Two IR spectrometer (PerkinElmer, model L160000A). Gel content and swelling measurements were conducted to determine the gel content and crosslinking density in the samples. All of the POGDA samples ($10 \times 5 \times 1.5 \text{ mm}^3$, number of specimen for each formulation, $n = 3$) were weighed [initial mass (W_0)] before immersion in acetone solvent at room temperature. After 24 h, the swollen specimens were removed and blotted with filter paper to remove excess solvent. The swollen specimens were placed in sealed vials and weighed to determine the swollen mass (W_s). After 3 days of drying at 60°C , the specimens were weighed again to obtain the dry mass (W_d). The gel content and the

Table I. Design Matrix of POGDA

Designation	Molar ratio		
	Oct	Gly	DA
POGDA (0.9 Gly)	0.1	0.9	1
POGDA (0.8 Gly)	0.2	0.8	1
POGDA (0.7 Gly)	0.3	0.7	1
POGDA (0.6 Gly)	0.4	0.6	1
POGDA (0.5 Gly)	0.5	0.5	1

swelling percentages were calculated according to the following equations:

$$\text{Gel content (\%)} = (W_d/W_0) \times 100 \quad (1)$$

$$\text{Swelling (\%)} = [(W_s - W_d)/W_d] \times 100 \quad (2)$$

The crosslinking density, (ν) was computed from the swelling properties with the Flory–Rehner equation^{29,30}:

$$\nu = \frac{-\ln[(1 - \nu_2) + \nu_2 + \chi \nu_2^2]}{V_s \left(\nu_2^{1/3} - \frac{2\nu_2}{f} \right)} \quad (3)$$

where ν_2 is the polymer volume fraction of the swollen sample, V_s is the molar volume of the solvent (molar volume of acetone = 74 cm³/mol),³¹ and χ is the polymer–solvent interaction parameter. A value of $\chi = 0.38$ was calculated for this study, and the details of calculation were discussed in a previous article.³²

Thermal Properties

Differential scanning calorimetry (DSC) was performed with a Mettler Toledo DSC 882e to determine the T_m values of the POGDA polymers with 8–13-mg samples encapsulated in aluminum pans. The samples were heated under nitrogen gas from 30 to 100 °C, cooled to –50 °C, and then heated again to 100 °C at a heating/cooling rate of 10 °C/min.

Transmittance Study

Optical transmittances of the POGDAs ranging from 200 to 800 nm were determined by ultraviolet–visible (UV–vis) spectroscopy (Shimadzu UV-3101PC, Japan) at room temperature. The sample thickness was 1.5 ± 0.08 mm.

Study of Crystallinity

X-ray diffraction (XRD) patterns were obtained with an XRD diffractometer (Rigaku Miniflex II) with Cu K α radiation (wavelength = 1.54 Å) at 40 kV and 30 mA. Patterns were recorded in the region of 2θ from 5 to 60°. The polymer crystallinity percentages were calculated with eq. (4) and Bragg's law³³ [eq. (5)] and were used to determine the interplanar distances of different peaks:

$$\text{Crystallinity percentage} = [A_c/(A_a + A_c)] \times 100\% \quad (4)$$

$$\text{Interplanar distance} = n\lambda/(2 \sin \theta) \quad (5)$$

where A_c is the area of the crystalline peak, A_a is the area of the amorphous peak, n is the order of diffraction ($n = 1$), λ is the X-ray wavelength, and θ is Bragg's angle.

In Vitro Biodegradation Testing

The *in vitro* biodegradation rates of the POGDA samples were measured by determination of changes in dry weight. The specimens ($1 \times 1 \times 0.15$ cm³, $n = 3$) were weighed and immersed into phosphate-buffered saline at 37 °C for 60 days. The weight loss was calculated with eq. (6) by comparison of the initial weight (W_i) and the dried weight (W_d). Phosphate-buffered saline was changed regularly to maintain a pH of 7:

$$\text{Weight loss (\%)} = [(W_i - W_d)/W_i] \times 100 \quad (6)$$

Shape-Memory Assessment

Bending tests used previously^{34,35} were adapted to evaluate the shape-memory properties of POGDA. The specimens ($2.5 \times 0.5 \times 0.15$ cm³, $n = 3$) were heated to 60 °C and then folded in half to deform to initial angle (θ_0). The deformed samples were quenched at –20 °C for 30 min. After external force was released, the deformed angle (θ_i) was recorded. The specimens were again heated to 60 °C at a heating rate of 2.5 °C/min, and changes in angle θ_f were recorded. Three cycles were repeated for each specimen. The fixity and recovery percentages were calculated with the following equations:

$$\text{Fixity (\%)} = (\theta_i/\theta_0) \times 100 \quad (7)$$

$$\text{Recovery (\%)} = [(\theta_i - \theta_f)/\theta_i] \times 100 \quad (8)$$

In Vitro Cytotoxicity Testing

Cytotoxicity tests were performed according to ISO 10993-5:2009, and specimens were prepared according to ISO 10993-12:2012. All of the specimens were sterilized under UV radiation for 20 min for both the top and bottom surfaces. We obtained the extraction fluids by soaking the specimens in Dulbecco's modified Eagle's medium (GIBCO, 1% PenStrep, 10% FBS) for 24 h at 37 °C with 5% CO₂ in an incubator with a ratio of 3 cm²/mL. The negative control media was prepared by incubated Dulbecco's modified Eagle's medium at 37 °C with 5% of CO₂ for 24 h. Human skin fibroblast 1184 (HSF 1184; passage 13) was seeded into a 96-well plate at a density of 1×10^5 cells/mL and incubated for 24 h at 37 °C with 5% CO₂. The fibroblast cells were exposed to the extraction fluids and the negative control media. The 96-well plate was incubated for an additional 24 h. At the end of the incubation period, a 3-(4,5-dimethylthiazol-2-yl)-2,5-diphenyltetrazolium bromide (MTT) assay was carried out to determine the cell viability with eq. (9) with a spectrophotometric microplate reader (ELx808) at 570 nm:

$$\text{Cell viability (\%)} = \left(\frac{\text{Sample absorbance}}{\text{Negative control absorbance}} \right) \times 100 \quad (9)$$

In Vitro Cell Proliferation Testing

Cell proliferation was analyzed under an inverted microscope (Zeiss, Axiovert100) equipped with a camera (Zeiss, AxioCam-ERc5s) and direct cell counting. HSF 1184 cells were seeded onto a 24-well plate with test samples at a density of 8×10^3 cells/mL. The test specimens were sterilized under UV radiation for 20 min for both the top and bottom surfaces, and they covered approximately one tenth of the cell layer surface. After the 24-well plate was incubated overnight at 37 °C with 5% CO₂, the cell morphology was examined under the inverted microscope, and the morphologies between days 1 and 4 were compared. On day 4, the end of incubation period, the cells at each well were

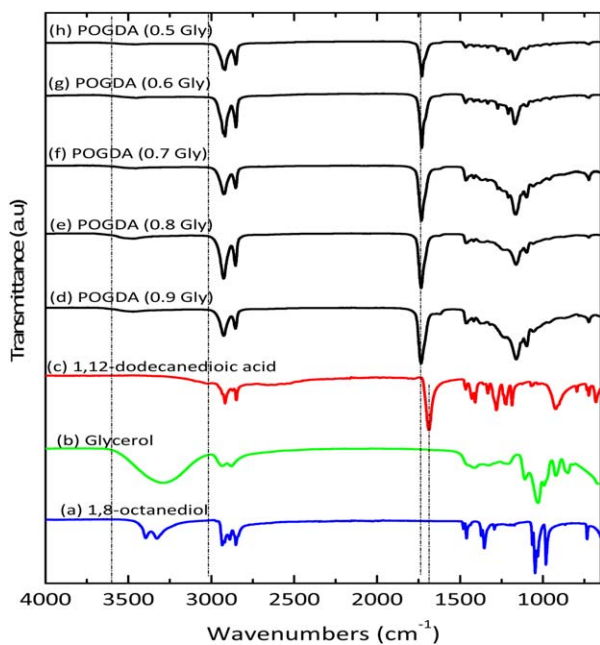


Figure 1. FTIR spectra of (a) Oct, (b) Gly, (c) DA, and POGDA with Oct/Gly/DA molar ratios of (d) 0.1:0.9:1, (e) 0.2:0.8:1, (f) 0.3:0.7:1, (g) 0.4:0.6:1, and (h) 0.5:0.5:1. [Color figure can be viewed in the online issue, which is available at wileyonlinelibrary.com.]

detached with TrypLE Express enzyme (GIBCO) and counted on a hemocytometer. The medium was changed every 2 days.

Statistical Analysis

The results in this article are expressed as the mean plus or minus the standard deviation. Data obtained by *in vitro* experiments were analyzed with one-way analysis of variance and Tukey *post hoc* tests with OriginPro software. Differences between groups with $p < 0.05$ were considered statistically significant.

RESULTS AND DISCUSSION

Structural Analysis

Figure 1 shows the FTIR spectra of the three monomers, Oct, Gly, and DA and the FTIR spectra of the POGDAs synthesized by polycondensation without solvent. The stretching shown in the range $3000\text{--}3600\text{ cm}^{-1}$ for Oct and Gly corresponded to O—H groups.³⁶ Broad absorption caused by the O—H groups in DA shifted to the region 3000 cm^{-1} because of the stronger hydrogen bonding between acid molecules. Observation in this region helped detect reactions between Oct, Gly, and DA. All of the spectra of POGDAs showed a similar trend. There was no significant peak in the region $3000\text{--}3600\text{ cm}^{-1}$ in the POGDA spectra; this indicated that the O—H groups in Oct and Gly almost disappeared in POGDA. A pronounced peak appearing in POGDA at 1736 cm^{-1} belonged to the carbonyl groups (C=O) in the esters.³⁷ DA C=O groups showed a peak at 1687 cm^{-1} . The shifting absorption band from 1687 to 1736 cm^{-1} further confirmed that the synthesis was successful. The stretching appearing at 2950 and 2850 cm^{-1} in all of the spectra was contributed by C—H bonds.

The gel content and swelling ratios are illustrated in Figure 2. All of the synthesized POGDAs showed 80–93% gel contents.

POGDA with the highest molar ratio of Gly showed a gel fraction of $93.1 \pm 0.9\%$. The lowest content of gel was found in POGDA (0.5 Gly) with a value of $80.1 \pm 0.7\%$. It is important to analyze the gel content in a thermoset polymer because the sol–gel content indicates the efficiency of crosslinking.^{38,39} The gel content is normally proportional to the degree of crosslinking. POGDA (0.9 Gly) was expected to contain the highest crosslinking density. The crosslinking density decreased when the amount of Gly decreased in the polymers. The swelling percentage of the POGDA polymers showed a different trend from that of the gel content, as shown in Figure 2. The swelling percentage in the POGDAs increased when the amount of Gly used in the polymers decreased. The crosslinking densities in the POGDAs were determined from the swelling properties and are summarized in Table II. On the basis of these results, the Oct/Gly molar ratio of 0.1:0.9 produced the POGDA with the highest crosslinking density value, and the crosslinking density values decreased gradually with decreasing molar ratios of Gly. POGDA (0.5 Gly) showed the lowest crosslinking density value, as expected. The molecular mass between crosslinks of POGDA (0.5 Gly) was calculated to be $1578 \pm 42\text{ g/mol}$, but it decreased to $670 \pm 13\text{ g/mol}$ for POGDA (0.9 Gly) because of crosslinking in the polymers, and similar results were found in other studies.^{40,41} The results from the gel content and swelling tests suggest that Gly acted as a crosslinking agent, as demonstrated in Figure 3. Three O—H groups in Gly reacted with DA to produce ester bonds and produce cross chains.

Thermal Data

To investigate the amorphous and crystalline properties of POGDAs, DSC was used to record thermographs of POGDA (0.9–0.5 Gly, Figure 4). Table II summarizes the thermal properties of the POGDAs. The curves in Figure 4(A) indicate the second heating run for all of the samples. The melting temperature (T_m) of POGDAs range from $12\text{--}40\text{ }^\circ\text{C}$ with POGDA (0.5 Gly) owned the highest T_m , which was $39.8\text{ }^\circ\text{C}$. The cooling curves of the POGDAs are shown in Figure 4(B). Crystallization temperatures (T_c) were found in all POGDA polymers, ranged from $-16\text{ }^\circ\text{C}$ to $9\text{ }^\circ\text{C}$. The endothermic melting peaks and exothermic crystallization peaks of POGDAs observed in Figure 4 revealed the existence of a

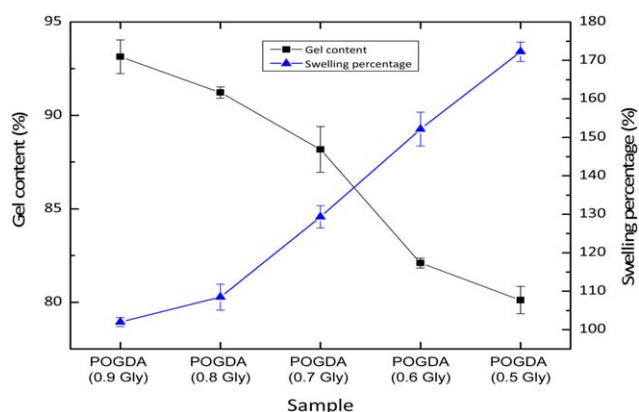


Figure 2. Gel contents and swelling percentages of POGDA (0.9 Gly), POGDA (0.8 Gly), POGDA (0.7 Gly), POGDA (0.6 Gly), and POGDA (0.5 Gly). [Color figure can be viewed in the online issue, which is available at wileyonlinelibrary.com.]

Table II. Physical and Thermal Properties of POGDA Polymers

Polymer	Density (g/cm ³)	ν , Crosslinking density (mol/m ³)	M_c (g/mol)	T_m (°C)	ΔH_m (J/g)	T_c (°C)	ΔH_c (J/g)
POGDA (0.9 Gly)	1.09 ± 0.01	1621 ± 32	670 ± 13	12.0	34.7	0.0	35.9
POGDA (0.8 Gly)	1.07 ± 0.06	1494 ± 81	725 ± 42	15.2	36.3	-4.9	36.1
POGDA (0.7 Gly)	1.08 ± 0.03	1084 ± 44	993 ± 40	21.1	31.9	-15.6, 6.1	41.8
POGDA (0.6 Gly)	1.06 ± 0.05	836 ± 45	1264 ± 66	28.9	53.65	-10.9, 2.4	53.1
POGDA (0.5 Gly)	1.05 ± 0.05	668 ± 18	1578 ± 42	39.8	66.10	-7.2, 9.4	70.1

M_c , molecular mass between crosslinks. ΔH_c , enthalpy of crystallization

crystallinity region in the polymer for all compositions; this indicated that POGDA was a semicrystalline polymer. As the content of Gly increased, the melting of polymer crystals shifted to lower temperatures and the enthalpy of melting (ΔH_m) decreased; this indicated that Gly hindered the crystallization process in POGDA. Crystallization can be initialized by a chain-folding conformation with flexible and linear chain molecules of sufficient length.⁴² With low contents of Gly, the crosslinking density and chain branches in the backbone of POGDA were expected to decrease, and the formation of flexible long aliphatic chains that were able to crystallize was expected to increase.

Transmittance Study

Figure 5 compared UV-vis spectroscopy among POGDAs. All POGDAs showed different transmittance values. To compare the transparency of POGDA, transmittance values were taken at 550 nm, the wavelengths where human eyes are the most sensitive.⁴³ As seen in Figure 5, POGDA (0.9 Gly) had the highest value of 63% followed by POGDA (0.8 Gly) at 55%. POGDA (0.7 Gly) and (0.6 Gly) had 51 and 38% transmission values, respectively. 30% of transmission, the lowest rate, was shown by POGDA (0.5 Gly). Transparency in POGDA reflects the structure of polymer chains and if they are amorphous or appreciable crystalline. When all wavelengths of visible light are able to be transmitted through an unmodified polymer, the polymer is transparent. When light is scattered, the polymer appears milky; this shows that the polymer has a crystalline region in addition

to an amorphous region.⁴⁴ The results of UV-vis spectroscopy demonstrated that POGDA (0.9 Gly), POGDA (0.8 Gly), and POGDA (0.7 Gly) appeared as transparent polymers with transmittance values above 50% and T_m s lower than room temperature. POGDA (0.9 Gly) was relatively amorphous compared to the others because it had the closest transmittance value to poly(methyl methacrylate) (PMMA), a polymer which is highly amorphous with around 75% transparency.⁴⁵ POGDA (0.5 Gly) was relatively crystalline at room temperature, with a 30% transmittance value. The transparency of POGDA decreased with Gly content.

Study of the Crystallinity

The POGDA crystallinity was studied with XRD at ambient temperature. The XRD patterns for the POGDA samples are displayed in Figure 6. As shown in Figure 6, two different diffraction patterns were observed. For samples POGDA (0.9 Gly), POGDA (0.8 Gly), POGDA (0.7 Gly), and POGDA (0.6 Gly), their diffractograms revealed broad distributions in the 2θ range, centered at approximately $2\theta = 19.9^\circ$. These are the typical diffraction or scattering patterns for an amorphous solid.³³ Two sharp peaks were observed in the diffraction pattern of POGDA (0.5 Gly) at $2\theta = 21.4$ and 23.8° . These peaks corresponded to the reflection of X-rays hitting the crystal planes in POGDA (0.5 Gly). The POGDA (0.9 Gly)–POGDA (0.6 Gly) polymers showed amorphous characteristics at ambient temperature. POGDA (0.5 Gly) revealed its semicrystalline nature by showing crystalline peaks upon the amorphous peaks in its diffraction pattern. With Bragg's law, the distances between adjacent crystal planes (d -spacing) in POGDA (0.5 Gly) were calculated to be 4.147 Å for $2\theta = 21.4^\circ$ and 3.734 Å for $2\theta = 23.8^\circ$. The crystallinity of POGDA (0.5 Gly) was calculated to be 14.9% with eq. (4). The study of the POGDA crystallinity with XRD confirmed this study's hypothesis. POGDA (0.5 Gly) possessed crystalline regions at ambient temperature because of its high T_m . POGDAs with T_m s lower than ambient temperature, such as POGDA (0.9 Gly), POGDA (0.8 Gly), and POGDA (0.7 Gly), did not show diffraction peaks on their diffractograms. POGDA (0.6 Gly) had a T_m value close to ambient temperature (25–27°C) and failed to show diffraction peaks because the very low amount of crystalline regions remaining in the polymer after the melting of the crystallinity region across a wide range of temperatures, as shown in the DSC curves. We concluded that Gly acted as a crosslinking agent that hindered the crystallization process of POGDA.

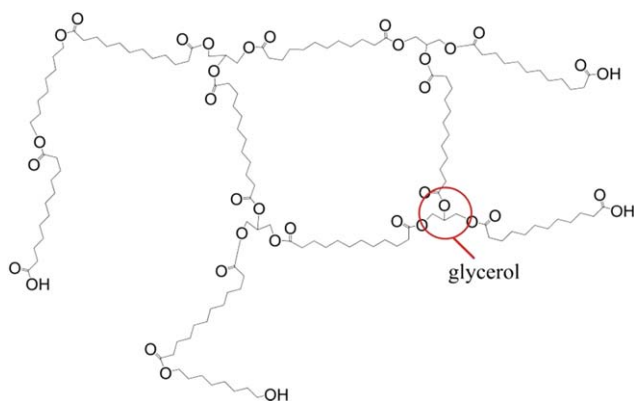


Figure 3. Possible network structure of POGDA with Gly acting as a crosslinking agent. [Color figure can be viewed in the online issue, which is available at wileyonlinelibrary.com.]

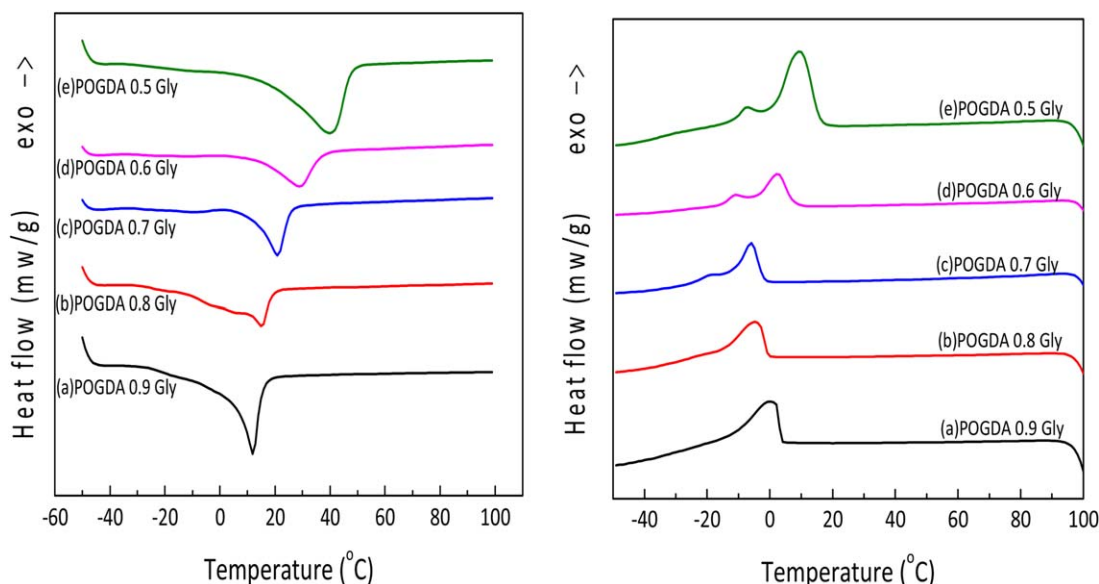


Figure 4. (A) DSC graphs of the second heating run for (a) POGDA (0.9 Gly), (b) POGDA (0.8 Gly), (c) POGDA (0.7 Gly), (d) POGDA (0.6 Gly), and (e) POGDA (0.5 Gly). (B) DSC graphs of the cooling run for (a) POGDA (0.9 Gly), (b) POGDA (0.8 Gly), (c) POGDA (0.7 Gly), (d) POGDA (0.6 Gly), and (e) POGDA (0.5 Gly). [Color figure can be viewed in the online issue, which is available at wileyonlinelibrary.com.]

In Vitro Biodegradation Properties

The *in vitro* degradation of the POGDAs was investigated by the monitoring of the weight loss during immersion in phosphate-buffered saline at 37 °C, and the results are shown in Figure 7. With a hydrolytically cleavable ester linkage as a backbone, POGDA was degradable via hydrolysis. At the beginning of testing, the weight loss increased rapidly for all of the samples and slowed after 2 weeks. No significant difference in the weight loss was observed for any of the samples for the first 2 weeks. After 2 weeks, POGDA (0.6 Gly) and POGDA (0.5 Gly) degraded more rapidly than the other samples. During the 60-day testing period, POGDA (0.9 Gly) lost the least weight, about $8.0 \pm 0.3\%$; this was followed by POGDA (0.8 Gly), which had a weight loss of $8.2 \pm 0.7\%$. Previous studies have shown that degradation rates can be influenced by various factors, including the material composition, hydrophobicity, and

crosslinking density of the polymer under the same environmental conditions.^{22,46} As expected, POGDA (0.9 Gly) showed the lowest weight loss because it contained the highest crosslinking density. A higher crosslinking in POGDA suggested that the number of bonds that could be broken to produce lower molecular weight products that were water-soluble increased. Similar trends have been reported in previous studies; when the composition of the polymer is the same, the degradation rate is affected mainly by the effect of the crosslinking density.^{39,47} POGDA (0.5 Gly) had the lowest crosslinking and degraded the most in 60 days, although its crystallinity should have slowed down the time for the water molecules to attack its backbone. The effect of the crosslinking density was dominant in the degradation rate of the POGDAs.

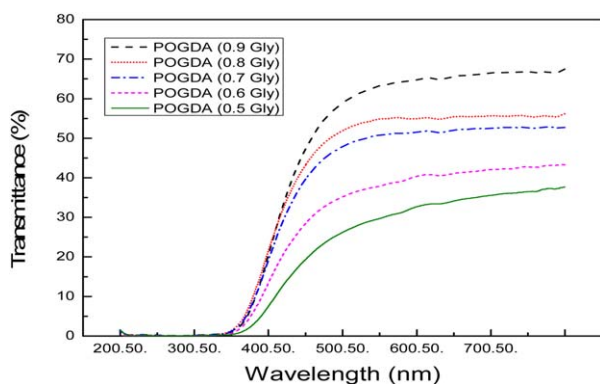


Figure 5. Visible light transmittance of POGDA (0.9 Gly), POGDA (0.8 Gly), POGDA (0.7 Gly), POGDA (0.6), and POGDA (0.5 Gly). [Color figure can be viewed in the online issue, which is available at wileyonlinelibrary.com.]

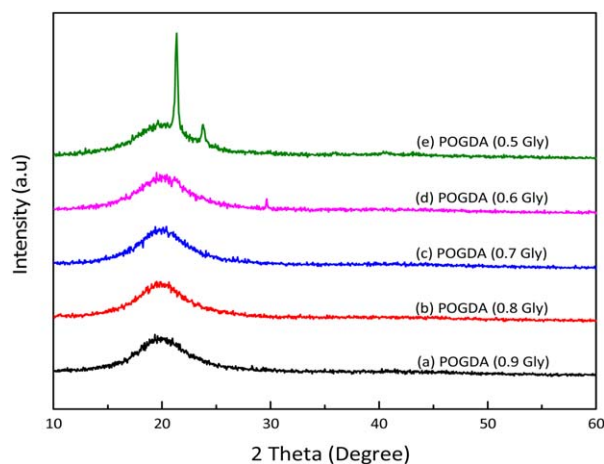


Figure 6. XRD diffraction patterns of (a) POGDA (0.9 Gly), (b) POGDA (0.8 Gly), (c) POGDA (0.7 Gly), (d) POGDA (0.6 Gly), and (e) POGDA (0.5 Gly). [Color figure can be viewed in the online issue, which is available at wileyonlinelibrary.com.]

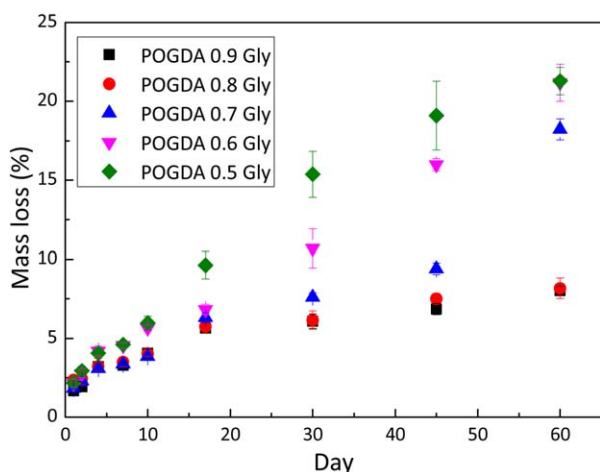


Figure 7. Degradation rates of POGDA (0.9–0.5 Gly) as the mass loss (%) versus the time (days). [Color figure can be viewed in the online issue, which is available at wileyonlinelibrary.com.]

Shape-Memory Behavior

The shape-memory behavior of POGDA (0.5 Gly) was determined with a simple bending test and is demonstrated in Figure 8. The fixity rate of POGDA (0.5 Gly) was approximately 100%. We observed in Figure 8 that around 24 °C, the deformed sample started to recover its permanent shape. The sample regained 50% of its permanent shape at approximately 32 °C. When the T_m (39.8 °C) of POGDA (0.5 Gly) was reached, the polymer recovered 95% of its original shape and fully recovered around 43 °C. The recovery behavior shown by POGDA (0.5 Gly) was an S shape. It recovered slowly below 30 °C, accelerated above 30 °C, and decreased at 95% recovery. POGDA (0.5 Gly) showed a 100% recovery ability at the end of the test. For a polymer to have a shape-memory effect, it has to contain hard and soft segments in its structure. The hard segment determines the permanent shape of the polymer, and the soft segment contributes to the temporary shape of the polymer.^{35,48} Among the synthesized POGDAs, only POGDA (0.5 Gly) displayed temperature-sensitive shape-memory behavior by maintaining a temporarily

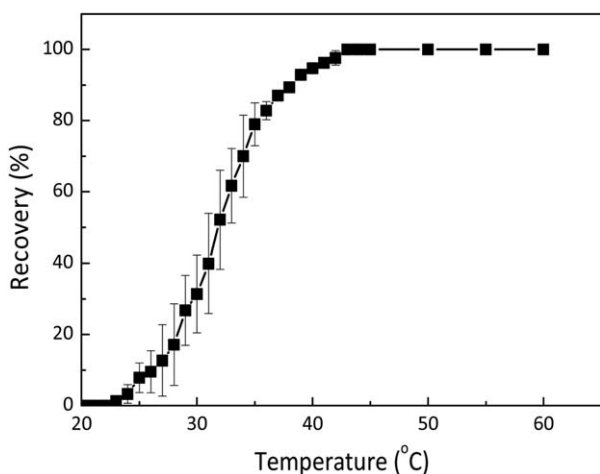


Figure 8. Shape-memory behavior of POGDA (0.5 Gly) at temperatures of 20–60 °C.

deformed shape and recovering its permanent shape upon heating. Other samples were unable to maintain a temporarily deformed shape because of a lack of crystallinity in their polymer structure to act as a soft segment. POGDA (0.5 Gly) had the highest degree of crystallization and showed better shape-memory behavior than the other samples. POGDA (0.5 Gly) was deformed to a temporary shape at –20 °C, where the crystallization process occurred, and was able to retain the deformation at temperatures lower than its T_m . Crystallization in POGDA (0.5 Gly) never reached 100%, but it was sufficient to prevent the sample from recovering to its permanent shape immediately after the external force was removed. The recovery of the polymer occurred between 24 and 43 °C. As the heating process continued, decreasing amounts of crystallites were present to maintain the deformed shape, and eventually POGDA (0.5 Gly) recovered to its permanent shape, as defined by its covalent crosslinked points.³⁴ The results prove that POGDA (0.5 Gly) contained sufficient hard segments to recover from deformation to its original shape.

In Vitro Cytotoxicity Testing

Human skin fibroblasts were used to perform an *in vitro* cytotoxicity assessment as an initial screening of the biocompatibility of the synthesized polyester. The quantitative MTT assessment results are displayed in Figure 9. All of the samples were cultured in 100% extraction fluid and compared to cells cultured as a negative control. All of the POGDAs showed cell viabilities of 70% or greater. There was no significant difference between the five samples ($p > 0.05$). The samples showed low cytotoxic potentials and, by ISO 10993-5:2009 standards, were potentially biocompatible.

In Vitro Cell Proliferation Testing

A preliminary investigation of the biocompatibility of the POGDAs was conducted with fibroblast cells without any treatment of the polymers. The impact of the POGDA polymers on fibroblasts is shown in Figures 10 and 11. As shown in Figure 10(A), cells cultured with the POGDAs exhibited multipolar or bipolar shapes regardless of the monomer composition. HSF 1184 cells exposed to the POGDAs adopted the same healthy, well-spread,

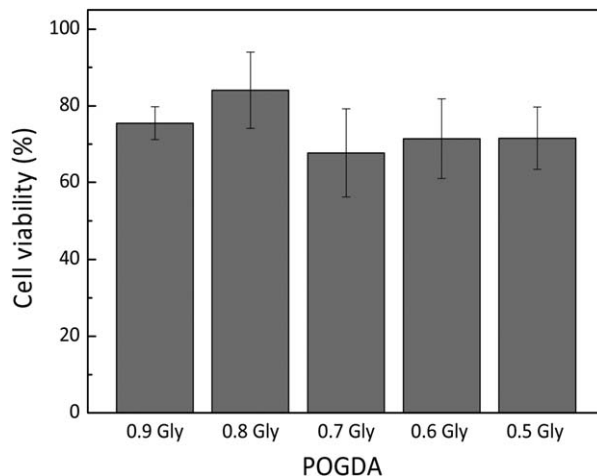


Figure 9. MTT assay of human skin fibroblasts cultured with the extraction fluid from POGDA (0.9 Gly–0.5 Gly) for 24 h.

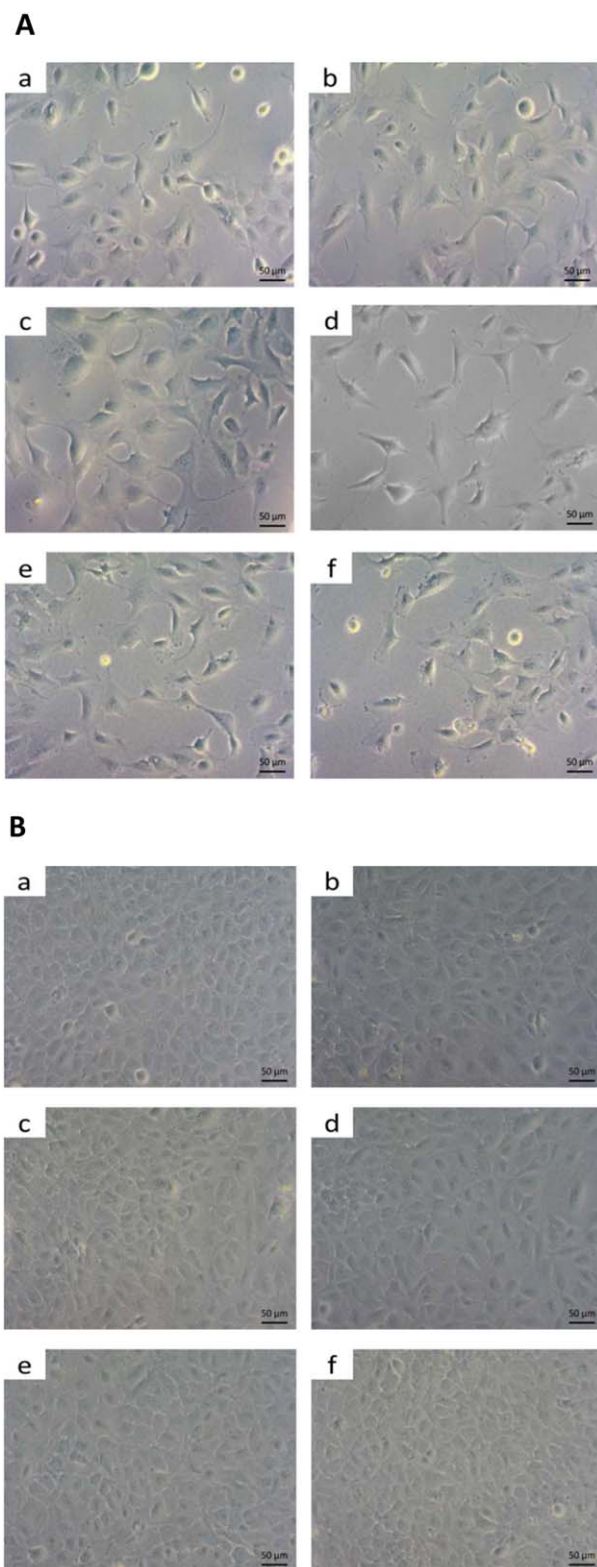


Figure 10. (A) Cell pictures on day 2: (a) negative control, (b) POGDA (0.9 Gly), (c) POGDA (0.8 Gly), (d) POGDA (0.7 Gly), (e) POGDA (0.6 Gly), and (f) POGDA (0.5 Gly). (B) Cell pictures on day 4: (a) negative control, (b) POGDA (0.9 Gly), (c) POGDA (0.8 Gly), (d) POGDA (0.7 Gly), (e) POGDA (0.6 Gly), and (f) POGDA (0.5 Gly). [Color figure can be viewed in the online issue, which is available at wileyonlinelibrary.com.]

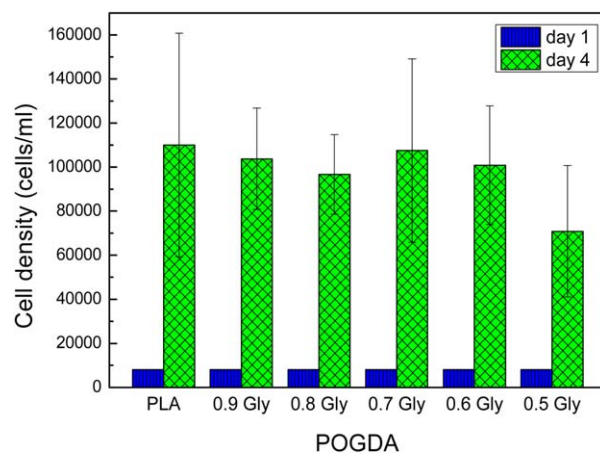


Figure 11. Cell density of PLA and POGDA polymers on the first and fourth days of the incubation period. [Color figure can be viewed in the online issue, which is available at wileyonlinelibrary.com.]

and spindle-like shape as the negative control cells. All cells were elongated and ready to proliferate. Figure 10(B) illustrates the cell conditions on day 4. The fibroblast cells were fully confluent in each well for all of the test samples, and similar cell morphologies were found. Direct cell counting was carried out on day 4 to determine cell growth rate, and the results are displayed in Figure 11. After 4 days of incubation, the cell densities in all of the wells had increased by at least 10 times. The growth rates of the cells between the PLA and POGDA samples were not significantly different.

CONCLUSIONS

POGDAs, biodegradable polyesters composed of monomers from renewable resources, were synthesized in this study with a solvent-free method. The results for gel content, swelling, UV-vis spectroscopy, DSC, XRD patterns, and biodegradation show that the properties of the POGDAs could be fine-tuned through variations in the molar ratio of the reactants. A shape-memory effect for POGDA was achieved by alterations in the crosslinking density and crystallinity to obtain hard and soft segments that remembered permanent and temporary shapes. The *in vitro* cytotoxicity and *in vitro* cell proliferation tests confirmed that the POGDAs have great potential for use in biomedical applications, such as scaffolds in tissue engineering.

ACKNOWLEDGMENTS

This work was funded by the Universiti Teknologi Malaysia (Tier 1 Research University Grant 06H48). The authors acknowledge Fad-zilah Adibah Abdul Majid and the Tissue Culture Engineering Research Group for the cell culture room facility.

REFERENCES

1. Moukwa, M. *JOM J. Miner. Met. Mater. Soc.* **1997**, *49*, 46.
2. Nair, L. S.; Laurencin, C. T. *Prog. Polym. Sci.* **2007**, *32*, 762.
3. Erbel, R.; Di Mario, C.; Bartunek, J.; Bonnier, J.; de Bruyne, B.; Eberli, F. R.; Erne, P.; Haude, M.; Heublein, B.;

- Horrigan, M.; Ilsley, C.; Böse, D.; Koolen, J.; Lüscher, T. F.; Weissman, N.; Waksman, R. *Lancet* **2007**, 369, 1869.
4. Griffith, L. G. *Acta Mater.* **2000**, 48, 263.
5. Furth, M. E.; Atala, A.; Van Dyke, M. E. *Biomaterials* **2007**, 28, 5068.
6. Garg, T.; Singh, O.; Arora, S.; Murthy, R. *Critical ReviewsTM in Therapeutic Drug Carrier Systems* **2012**, 29, 1.
7. Lendlein, A.; Neffe, A. T.; Pierce, B. F.; Vienen, J. *Int. J. Artif. Org.* **2011**, 34, 71.
8. Yin, J.; Luan, S. *Regen. Biomater.* **2016**, 3, 129.
9. Liu, X.; Ma, P. *Ann. Biomed. Eng.* **2004**, 32, 477.
10. Shah Mohammadi, M.; Bureau, M. N.; Nazhat, S. N. In *Biomedical Foams for Tissue Engineering Applications*; Netti, P. A., Ed.; Woodhead: Cambridge, MA, **2014**.
11. Barrett, D. G.; Yousaf, M. N. *Molecules* **2009**, 14, 4022.
12. Seyednejad, H.; Ghassemi, A. H.; van Nostrum, C. F.; Vermonden, T.; Hennink, W. E. *J. Controlled Release* **2011**, 152, 168.
13. Wang, Y.; Ameer, G. A.; Sheppard, B. J.; Langer, R. *Nat. Biotechnol.* **2002**, 20, 602.
14. Bruggeman, J. P.; de Bruin, B.-J.; Bettinger, C. J.; Langer, R. *Biomaterials* **2008**, 29, 4726.
15. Lei, L.; Ding, T.; Shi, R.; Liu, Q.; Zhang, L.; Chen, D.; Tian, W. *Polym. Degrad. Stabil.* **2007**, 92, 389.
16. Ajili, S. H.; Ebrahimi, N. G.; Soleimani, M. *Acta Biomater.* **2009**, 5, 1519.
17. Alvarado-Tenorio, B.; Romo-Urbe, A.; Mather, P. T. *Macromolecules* **2015**, 48, 5770.
18. Yang, X.; Cui, C.; Tong, Z.; Sabanayagam, C. R.; Jia, X. *Acta Biomater.* **2013**, 9, 8232.
19. Guo, B.; Chen, Y.; Lei, Y.; Zhang, L.; Zhou, W. Y.; Rabie, A. B. M.; Zhao, J. *Biomacromolecules* **2011**, 12, 1312.
20. Serrano, M. C.; Carbajal, L.; Ameer, G. A. *Adv. Mater.* **2011**, 23, 2211.
21. Li, H.; Sivasankarapillai, G.; McDonald, A. G. *Ind. Crops Prod.* **2015**, 67, 143.
22. Yang, J.; Webb, A. R.; Ameer, G. A. *Adv. Mater.* **2004**, 16, 511.
23. Solomon, B. O.; Zeng, A. P.; Biebl, H.; Schlieker, H.; Posten, C.; Deckwer, W. D. *J. Biotechnol.* **1995**, 39, 107.
24. Demirbaş, A. *Energy Conversion Manage.* **2003**, 44, 2093.
25. Wang, Z.; Zhuge, J.; Fang, H.; Prior, B. A. *Biotechnol. Adv.* **2001**, 19, 201.
26. Bertuzzi, A.; Mingrone, G.; Gaetano, A. D.; Gandolfi, A.; Greco, A. V.; Salinari, S. *Br. J. Nutr.* **1997**, 78, 143.
27. Park, H.; Lee, H.; Seo, J.; Kim, H. W.; Wall, I. B.; Gong, M. S.; Knowles, J. C. *Acta Biomater.* **2012**, 8, 2911.
28. Ayorinde, F. O.; Powers, F. T.; Streete, L. D.; Shepard, R. L.; Tabi, D. N. *J. Am. Oil Chem. Soc.* **1989**, 66, 690.
29. Flory, P. J. In *Principles of Polymer Chemistry*; Cornell University Press: Ithaca, NY, **1953**.
30. Gooch, J. W. In *Encyclopedic Dictionary of Polymers*; Gooch, J. W., Ed.; Springer: New York, **2011**, 315.
31. Hansen, C. M. In *Hansen Solubility Parameters: A User's Handbook*; CRC: Boca Raton, FL, **2007**.
32. Messori, M.; Degli Esposti, M.; Paderni, K.; Pandini, S.; Passera, S.; Riccò, T.; Toselli, M. *J. Mater. Sci.* **2013**, 48, 424.
33. He, B. B. In *Two-Dimensional X-ray Diffraction*; Wiley: Hoboken, NJ, **2009**.
34. Lendlein, A.; Kelch, S. *Angew. Chem. Int. Ed.* **2002**, 41, 2034.
35. Lin, J.; Chen, L. *J. Appl. Polym. Sci.* **1998**, 69, 1563.
36. Wade, L. G. In *Organic Chemistry*; Pearson Education: Upper Saddle River, NJ, **2010**; p 524.
37. Tang, J.; Zhang, Z.; Song, Z.; Chen, L.; Hou, X.; Yao, K. *Eur. Polym. J.* **2006**, 42, 3360.
38. Amsden, B. *Soft Matter* **2007**, 3, 1335.
39. Bettinger, C. J.; Bruggeman, J. P.; Borenstein, J. T.; Langer, R. *J. Biomed. Mater. Res. Part A* **2009**, 91, 1077.
40. Yang, J.; Webb, A. R.; Pickerill, S. J.; Hageman, G.; Ameer, G. A. *Biomaterials* **2006**, 27, 1889.
41. Li, H.; Sivasankarapillai, G.; McDonald, A. G. *J. Appl. Polym. Sci.* **2014**, 131, DOI: 10.1002/app.41103.
42. Cheng, S. Z. D.; Jin, S. In *Handbook of Thermal Analysis and Calorimetry*; Stephen, Z. D. C., Ed.; Elsevier Science: Amsterdam, **2002**, 167.
43. Liu, M.; Zhang, Y.; Wu, C.; Xiong, S.; Zhou, C. *Int. J. Biol. Macromol.* **2012**, 51, 566.
44. Solis, F. *Am. J. Phys.* **2003**, 71, 285.
45. Chen, W.; Feng, L.; Qu, B. *Solid State Commun.* **2004**, 130, 259.
46. Coneski, P. N.; Rao, K. S.; Schoenfish, M. H. *Biomacromolecules* **2010**, 11, 3208.
47. Barrett, D. G.; Luo, W.; Yousaf, M. N. *Polym. Chem.* **2010**, 1, 296.
48. Tcharkhtchi, A.; Abdallah-Elhirsati, S.; Ebrahimi, K.; Fitoussi, J.; Shirinbayan, M.; Farzaneh, S. *Polymers* **2014**, 6, 1144.